Journal of Systems Engineering and Electronics
Vol. 29, No. 4, August 2018, pp.723 – 730

GA-based approach to phase compensation of large phased array antennas

ZAHEDI Amir* and ABBASI ARAND Bijan

Department of Electrical and Computer Engineering, Tarbiat Modares University, Tehran 14115-111, Iran

Abstract: The investigation of the effect of electrical and mechanical errors on the performance of a large active phased array antenna is studied. These errors can decrease the antenna performance, for instance, the gain reduction, side lobe level enhancement, and incorrect beam direction. In order to improve the performance of the antenna in the presence of these errors, phase error correction of large phased array antennas using the genetic algorithm (GA) is implemented. By using the phase compensation method, the antenna overall radiation pattern is recovered close to the ideal radiation pattern without error. By applying the simulation data to a 32×40 array of elements with a square grid at the frequency of S-band and measurement of the radiation pattern, the effectiveness of the proposed method is verified.

Keywords: antenna, genetic algorithm (GA), phased array, radiating element.

DOI: 10.21629/JSEE.2018.04.07

1. Introduction

In modern radar systems, phased array antennas (PAAs) are extensively used. These antennas include many individual radiating elements. For large PAAs, the number of radiating elements may reach hundreds or even thousands.

Generally, PAAs are liable to two types of errors. The first type of errors is the mechanical errors which include random errors in element positions during fabrication and distortion in the array plane [1,2]. Structural deformations of the array can cause distortion of the antenna patterns. Specially, space-based systems are inclined to such antenna distortion due to the large antenna sizes and minimum weight necessities [3].

The second type of errors is the electrical ones which happen in the element amplitude and phase excitation and electric length error of each radio frequency (RF) channel [4].

In general, both mechanical and electrical errors introduce phase variations. Since the radiation pattern of the whole array is controlled by the relative phases between the elements, phase errors are an important issue in any PAA. Distortion of the relative phases can cause severe deterioration of the radiation pattern, such as broadening of the main beam, the increment of the side-lobe level or erroneous beam direction.

Until now many methods have been introduced to describe the coupling relationship between electrical/mechanical distortion error and electromagnetic performance of the PAA [1,5 – 9]. The effect of the random errors on the radiation performance of PAAs by the probability and statistics method was studied in [1]. To demonstrate the effect of the two different distortions on the electromagnetic (EM) performance of the antenna, a model on the position error of each radiating element in the bent plane and bowl-shape plane was developed in [5]. Other methods have been implemented to recover a high quality pattern from a distorted antenna [7]. However, according to our knowledge, the investigation of phase correction of a phased array with thousands of elements has not been examined yet. Automatic phase correction of PAAs using the genetic algorithm (GA) was presented in [10].

Therefore, in this paper, first we have a glance at the effect of two types of mentioned errors on the radiation performance of a large PAA. Then, by considering the large phased array with phase errors at each channel, the correction method described in [10] is implemented in this array in order to compensate the phase distribution of the antenna.

2. Investigation of errors in PAAs

2.1 Electrical errors

In order to analyze the effect of the electrical errors, it is assumed that the array has an amplitude error α_{mn} and phase error δ_{mn} at the (m, n)th element. The term related to amplitude error, α_{mn}, explains this fact that the signal at the (m, n)th element has amplitude $|A_{mn}|(1 + \alpha_{mn})$, where

Manuscript received April 30, 2017.
*Corresponding author.

$|A_{mn}|$ is the correct amplitude. The phase error δ_{mn} indicates that the accurate phase to direct a beam to the desired angle is not the correct excitation, but $\exp(j\delta_{mn})$ must be multiplied in the correct excitation. Furthermore, there are usually many failed elements (zero amplitude signal) in a typical array, which are placed across the array. These useless elements can be modeled by assuming a fixed probability P that any element is operating properly except for amplitude and phase errors, so that the probability of that element being completely failed is $(1-P)$ [3].

By considering the amplitude and phase errors, the far-field pattern function can be expressed as follows:

$$f(\theta,\phi)=\sum_{m=1}^{M}\sum_{n=1}^{N}A_{mn}\gamma_{mn}(1+\alpha_{mn})\mathrm{e}^{\mathrm{j}\delta_{mn}}\cdot$$
$$\exp\{\mathrm{j}k[md_xU+nd_yV]\} \tag{1}$$

with spherical polar coordinates as

$$\begin{cases}U=\sin\theta\cos\phi\\ V=\sin\theta\sin\phi\end{cases} \tag{2}$$

where $\gamma_{mn}=0$ or 1 for failed or invalid elements, α_{mn} and δ_{mn} are random amplitude and phase errors, A_{mn} is the complex excitation coefficient with amplitude $|A_{mn}|$ and phase φ_{mn}.

2.2 Mechanical errors

2.2.1 Distortion in array plane

Two common structural distortions are the bent and bowl-shape distortions shown in Fig. 1.

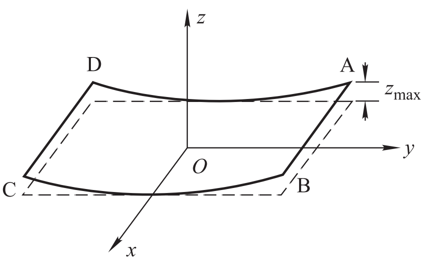

(a) Bent shape distortion

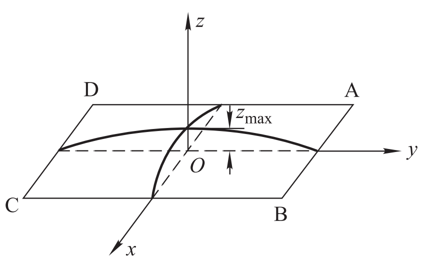

(b) Bowl shape distortion

Fig. 1 Distorted array plane of antenna [5]

By considering Fig. 1 and its mathematical aspects, the coordinate of the phase center of radiating elements in a bent plane can be specified as follows [5]:

$$z=z_{\max}\left(\frac{y}{y_{\max}}\right)^2 \tag{3}$$

where $y_{\max}$ is one-half of the length of the array aperture, and $z_{\max}$ is the maximum shift of the radiating elements in z direction. Consequently, the phase centers of the elements of the bowl plane are expected to be represented as follows:

$$z=z_{\max}\left(1-\frac{x^2}{x_{\max}^2}\right)\left(1-\frac{y^2}{y_{\max}^2}\right) \tag{4}$$

where $x_{\max}$ is also the half length of the array.

Consider a planar rectangular PAA like Fig. 1, whose number of radiating elements in the x-y plane is $M\times N$. Distortion of the relative phases can cause severe deterioration of the radiation pattern and must be considered in the array design.

As mentioned in [5], the structural distortion error of the radiating elements only influences the phase of the electric field of the element without changing the amplitude. Therefore, the effect of z-displacement of the elements from their ideal planar position is to present a surplus phase cause in the pattern function as

$$F(\theta,\phi)=\sum_{m=1}^{M}\sum_{n=1}^{N}A_{mn}\cdot$$
$$\exp\{\mathrm{j}k[md_xU+nd_yV+z_{mn}W]\} \tag{5}$$

$$\begin{cases}U=\sin\theta\cos\phi\\ V=\sin\theta\sin\phi\\ W=\cos\theta\end{cases} \tag{6}$$

where z_{mn} is the displacement of the radiating element (m,n) in z direction, A_{mn} is the complex excitation of each element, and k is the wave number.

2.2.2 Random errors in element positions

Due to assembling tolerance during antenna manufacturing, the position and orientation error of radiating elements is inevitable. These mechanical process errors of the array structure can induce major displacement of the radiating elements relative to each other.

Furthermore, when the PAA is mounted on a moving platform, the vibrations of the array structure may result in deformation of the antenna aperture or element position error.

Taking into account the random errors in element positions, the far-field radiation pattern [1] can be expressed as

$$F(\theta,\phi)=\sum_{m=1}^{M}\sum_{n=1}^{N}A_{mn}\cdot$$

$$\exp\{jk[x_{mn}U + y_{mn}V + z_{mn}W]\}. \quad (7)$$

In this expression, x_{mn}, y_{mn}, and z_{mn} are the coordinates of the mth element of the nth row now given as

$$\begin{cases} x_{mn} = md_x + \xi_{mn} \\ y_{mn} = nd_y + \eta_{mn} \\ z_{mn} = \zeta_{mn} \end{cases} \quad (8)$$

where ξ_{mn}, η_{mn}, and ζ_{mn} are the random errors assumed to be of normal distribution with zero average and standard deviation of σ.

3. Phase correction method

3.1 Theoretical background

For large PAAs, pattern degradation due to structural distortions can be modified by suitable phase compensation. The phase compensation for the (m, n)th element [1] can then be taken as

$$\varphi_{mn} = e^{-jkw_0 z_{mn}} \quad (9)$$

where $w_0 = \cos\theta_0$ is determined from the direction of the beam scan from (9). Therefore, error-free main beam is expected to be achievable.

By considering the $M \times N$ planar PAA, its far-field radiation pattern can be expressed as follows:

$$F(\theta, \phi) = \sum_{m=1}^{M}\sum_{n=1}^{N} A_{mn} \times \exp[j\varphi_{mn}^{\text{error}}]\cdot$$

$$f_{mn}(\theta, \phi) \times \exp\{jk[md_x U + nd_y V]\} \quad (10)$$

where $f_{mn}(\theta, \phi)$ is the antenna element pattern, $\varphi_{mn}^{\text{error}}$ is the antenna elements phase error that can be modeled by electrical or mechanical errors, and all other symbols have the same meaning as defined before.

In this paper, for phase error correction, the correction method introduced in [10] is used. Consider now the measurement arrangement for phase error correction as shown in Fig. 2. This arrangement corresponds to the two-antenna system recognized as Friis transmission formula (11) that relates the power transmitted P_t to the power received P_r between two antennas separated by a distance $R > 2D^2/\lambda$, where D is the largest dimension of whichever antenna [11].

$$P_r = P_t \times G_t \times G_r \times \left(\frac{\lambda}{4\pi R}\right)^2 \quad (11)$$

where G_t and G_r are the gain of transmitted and received antennas, respectively. The term $\left(\frac{\lambda}{4\pi R}\right)^2$ is the free-space loss factor.

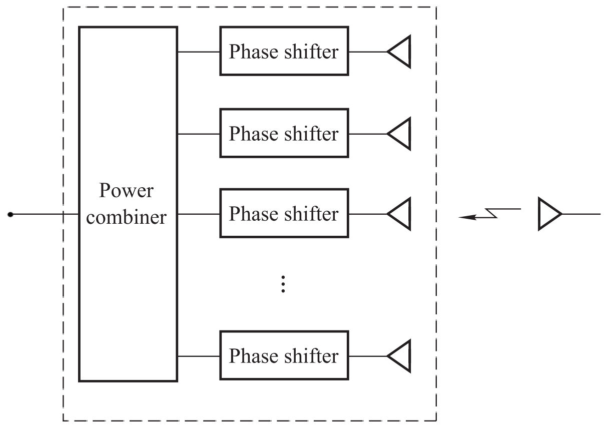

Fig. 2 Measurement configuration for phase error correction

According to Fig. 2, the PAA under correction is receiving a signal from a reference antenna. The objective of the problem is to maximize a fitness function with respect to correct phases φ_{mn} of the complex excitation coefficient A_{mn} for all i. In the receiving mode, optimal phases φ_{mn} are searched in a way that the receiving power P_r of the phased array is maximized by maximizing the receiving gain G_r of the PAA. The transmitting power P_t and gain G_t are provided by using the reference antenna. The fitness function in the receiving mode is depicted as below:

$$Fitness(\varphi_{mn}) = P_t \times G_t \times G_r(\theta, \phi) \times \left(\frac{\lambda}{4\pi R}\right)^2 \quad (12)$$

where R is the separation between the phased array and the reference antenna that is in such a way that far-field conditions fulfill.

In contrast, when the PAA under test is a transmitter, the optimal phases φ_{mn} are searched such that the receiving power P_r of the reference antenna is maximized by maximizing the transmitting gain G_t of the PAA. In order to find the optimal phases, the GA is applied. The GA is beneficial in optimization problems with numerous variables, especially in the case of large PAAs that the number of design variables is equal to the number of radiating elements.

3.2 Implementation of GA

In the case of the GA, an initial population of N_{pop} random candidate array phase distributions is generated and evolved for $MaxIt$ generations. More specifically, $\frac{N_{pop} \times P_c}{2}$ pairs of parents are chosen by the Rolletwheel selection at each iteration, where P_c is the crossover probability and in this paper has the value of 0.8. Each of these couples produces two children using crossover. Some agents may be mutated, to provide genetic diversity and enable the GA to search a wider space. Among all the individuals (parents plus children and mutated candidates), the best-scoring N_{pop} survives to the next generation, and the process repeats. The final array phase distribution is taken as the fittest individual after the specified number of iterations.

4. Simulation results

The analysis of the effect of electrical and mechanical errors on the performance of a PAA is presented in this section. The simulated antenna consists of 25×40 elements, the space within array elements is 0.5 times wavelength with the operating frequency of 9 GHz, and assume the excited current in the aperture is uniformly distributed.

By taking into account the amplitude and phase errors, and simultaneously the random errors in element positions, beam patterns have been computed and plotted for the planar array. Amplitude and phase errors are assumed to be of normal distribution with standard deviations of $\alpha = 0.1^\circ$, $\delta = 1^\circ$ respectively. The standard deviation of random errors is assumed to be $\sigma = \lambda/16$. The symbol σ represents the standard deviation of x, y, and z coordinates errors which are assumed to be equal and independent of each other. At the same time, in order to take into account a few failed elements in the array, the probability P is chosen to be 0.99.

Fig. 3 shows an example of calculated beam patterns of the planar array with the above amounts of random amplitude, phase and element position errors.

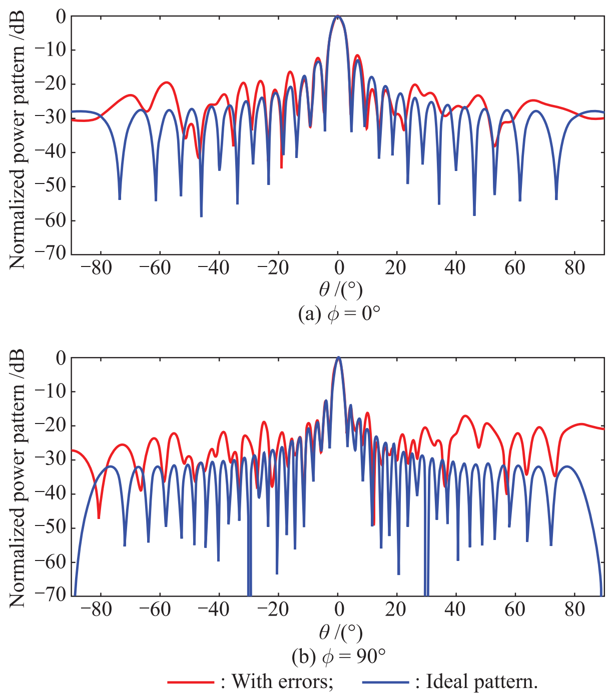

Fig. 3 Calculated beam pattern of the array with random errors

As can be seen, the random errors cause the increase of sidelobe levels and disruption of patterns' shapes.

In the next case, the simulation of distorted planar arrays has been done and in order to recover the radiation pattern to the ideal one, the mentioned algorithm has been applied in each case. In reality, the structural distortion error of PAA is usually small in the main beam region, and for example in the frequency of 9 GHz the typical distortion amount is about a few millimeters. Therefore, based on (5), the beam patterns for the distorted planar array with $z_{\max} = \lambda/16$ have been computed and corrected. Fig. 4 and Fig. 5 show the pattern cuts in the principal planes $\phi = 0$, and $\phi = 90^\circ$.

By comparing the three radiation patterns in each case, it is evident that both of the two distortions of the array plane have caused a disruption in the radiation pattern. With $\phi = 0^\circ$, for the bent shape distortion of array with $z_{\max} = \lambda/16$, the gain loss is 1.12 dB, and the maximum beam direction of antenna with $\phi = 90^\circ$ has a deviation of 1° and the sidelobe level of the antenna has been increased.

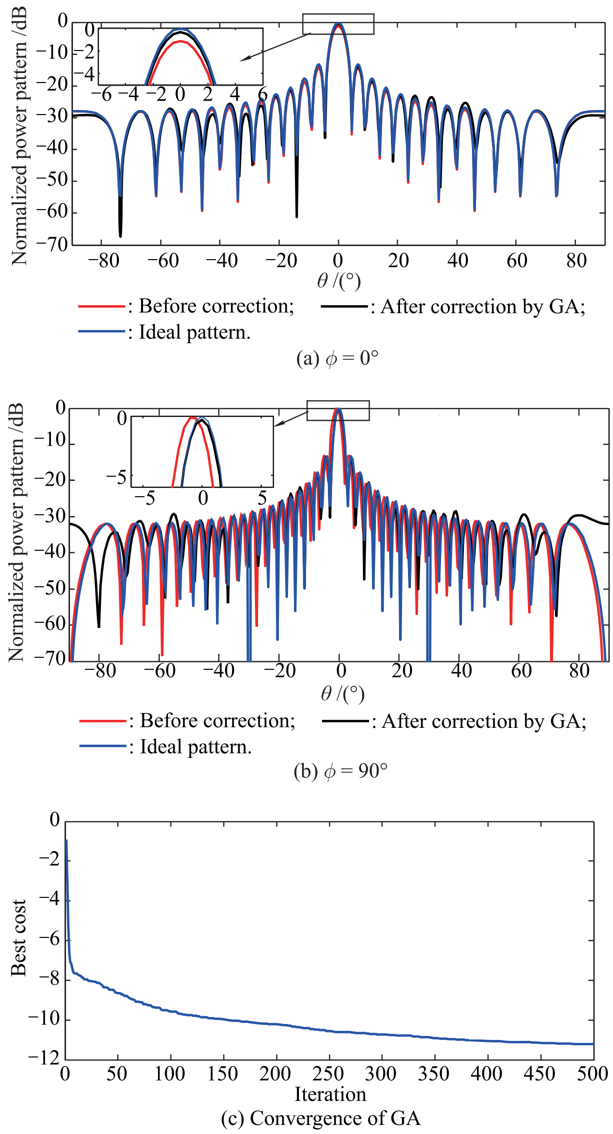

Fig. 4 Beam pattern of the array with bent-shape distortion

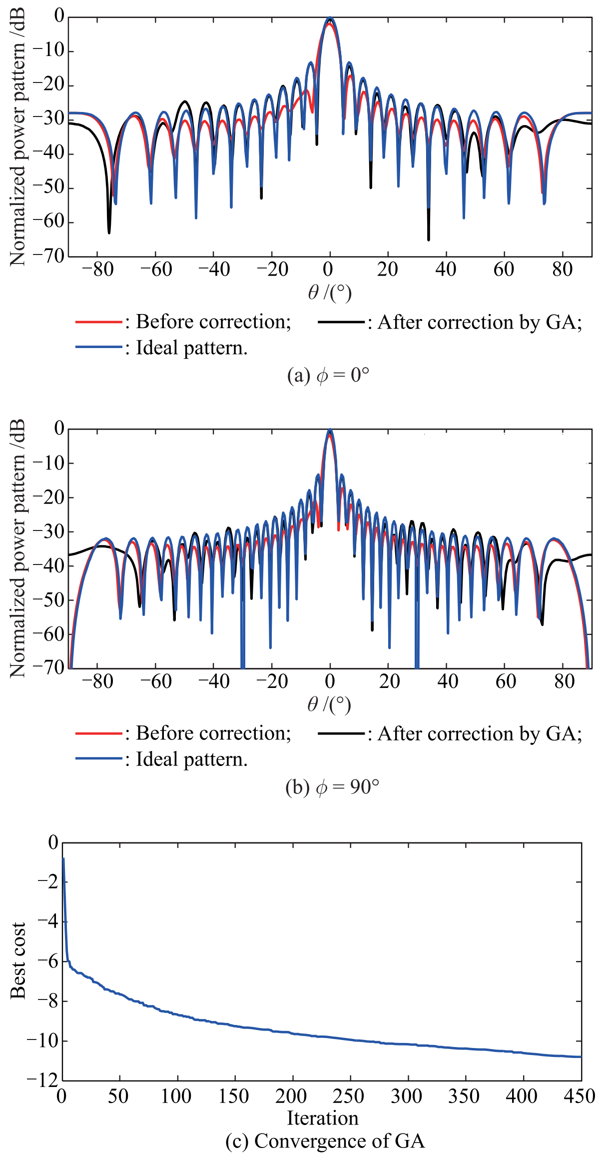

Fig. 5 Beam pattern of the array with bowl-shape distortion

As depicted in Table 1, after correction there is approximately no gain loss and no beam deviation and the radiation pattern is similar to the ideal pattern. HPBW represents half-power bean-width.

Table 1 Antenna performances before and after correction with bent-shape distortion

Operation	Gain enhancement after correction/dB	Gain reduction before correction/dB	HPBW after correction/(°)	HPBW before correction/(°)
$\phi = 0°$	0.78	−1.12	3.74°	4.61°
Operation	Beam deviation after correction	Beam deviation before correction	HPBW after correction/(°)	HPBW before correction/(°)
$\phi = 90°$	0	1°	2.33°	2.48°

For the same numerical value of the bowl shape distortion, the gain loss of the antenna with two azimuths is equal and about 2 dB as mentioned in Table 2. The beam deviation in both planes before correction is 0.5°. After correction the disrupted patterns have been improved, and the gain loss and the beam deviation have been compensated.

Table 2 Antenna performances before and after correction with bowl-shape distortion

Operation	Gain enhancement after correction/dB	Gain reduction before correction/dB	HPBW after correction/(°)	HPBW before correction/(°)
$\phi = 0°$	1.5	−2	3.74	4.61
$\phi = 90°$	1.5	−2	2.24	2.84

Note, in order to show the gain reduction, the radiation patterns in Fig. 4 and Fig. 5 are normalized to the maximum of the pattern in undistorted cases ($z_{\max} = 0$).

5. Experimental results

In order to verify the effectiveness of the proposed algorithm, a large PAA consisting of 32×40 elements is simulated and tested. The configuration of one subarray of this large phased array is shown in Fig. 6. The space within array elements is 0.5 times of the wavelength. The phase of the elements is controlled by four-bit digital phase shifters that are located behind each element.

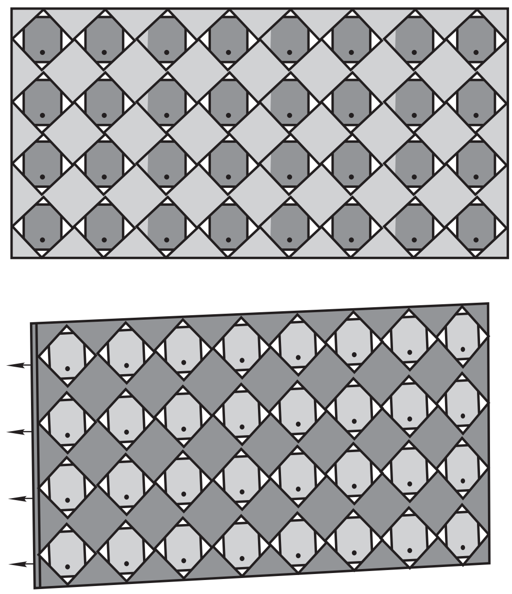

Fig. 6 Configuration of one subarray of the phased array

Each element is a coaxial feed-type microstrip patch. In order to increase the ability of electronic scanning of the array and to decrease the mutual coupling, each element is printed on RO4003 substrate with 20 mil thickness, and then it is placed on a separate spacer (interlaced Teflon) so that their substrates do not connect to each other physically. This can reduce the surface waves and prevent the unwanted modes propagation in the direction of antenna ground that results in the decrease of coupling between the elements.

Placing the printed patch on a spacer with high thickness can enhance the impedance bandwidth, but at the same time it can increase the inductive effect of the feeding probe and cause unwanted radiation. By designing a printed disk with capacitive effect under the substrate, this issue can be modified.

The phase errors of the array elements are measured and applied to the algorithm. In the GA, an initial population of $N_{pop} = 1\,500$ random candidate array phase distributions is generated and evolved for $MaxIt = 5\,000$ generations (7 501 500 number of function evaluations). The final array phase distribution is taken as the fittest individual after the specified number of iterations. Fig. 7 shows the simulation results of the radiation pattern before and after phase error correction, which are compared to the ideal pattern. As can be seen, the phase errors have caused a deep null in the main beam area and severe increase in sidelobe regions. By applying the phase error correction we expect to achieve a radiation pattern close to the ideal pattern without error. As can be seen from the result, after correction the consequent pattern (black curve) is highly analogous to the ideal radiation pattern (blue curve) with uniform distribution and error free.

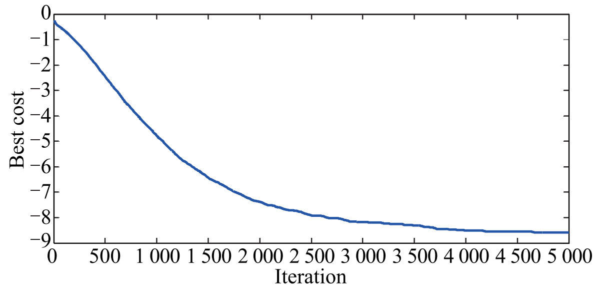

(c) Convergence of GA

Fig. 7 Simulation results of the radiation pattern

After correction, there are some residual of phase errors which have negligible standard deviation. That is why the peak sidelobe levels (PSLs) as depicted in Table 3 are less than – 13.2 dB in one side of the main beam and more than – 13.2 dB in other side of the main beam comparing with the uniform amplitude radiation pattern.

Table 3 Antenna performances before and after correction with and without scanning angle

Operation	Side-lobe level after correction/dB	HPBW after correction/(°)
$\phi = 0°, \theta_0 = 0°$	– 12.78/ – 13.7	2.8
$\phi = 90°, \theta_0 = 0°$	– 12.47/ – 13.91	2.3
$\phi = 0°, \theta_0 = 30°$	– 12.78/ – 13.68	3.2
$\phi = 90°, \theta_0 = 30°$	– 12.48/ – 13.92	2.67

Phase compensation becomes more of a challenge if the array's main beam is scanned. Fig. 8 shows the phase error correction results when the peak of the main beam is 30° away from the boresight.

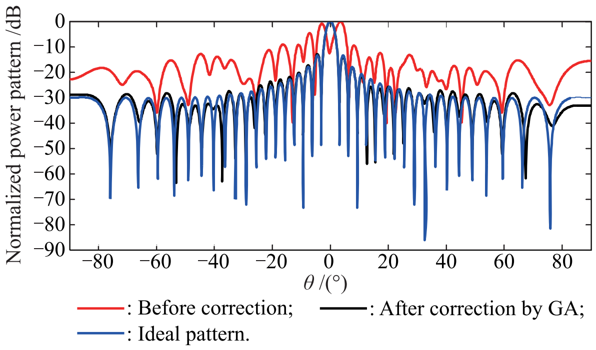

(a) $\phi = 0°$

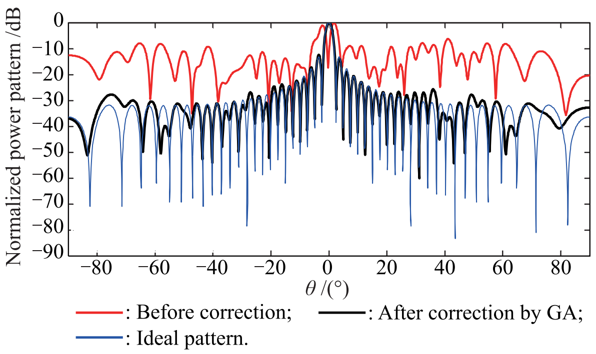

(b) $\phi = 90°$

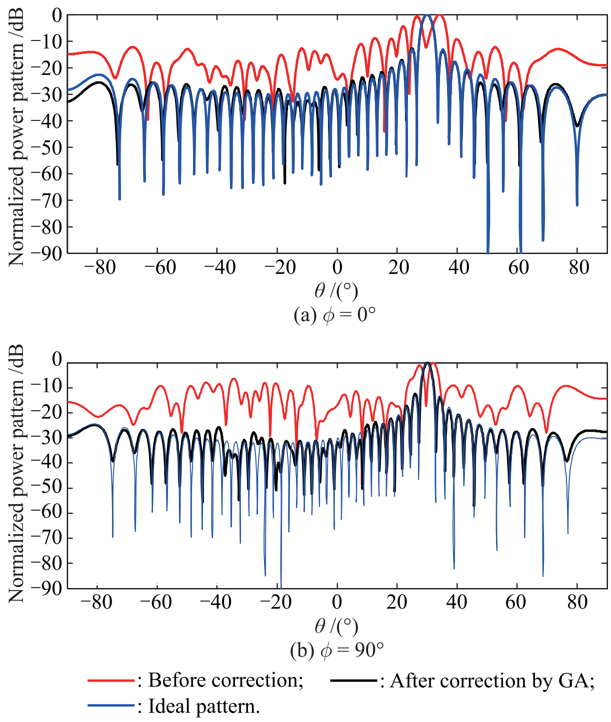

Fig. 8 Simulation results of the radiation pattern before and after correction at the 30° scan angle

It can be noticed that although the array's main beam is scanned, the radiation pattern still has the identical form of the ideal one that proves the effectiveness of the phase compensation method.

The antenna performances are depicted in Table 3 in both cases of scanning and not scanning the array main beam. The phase error causes the drastic increase of sidelobe levels in both cases. The desirable levels of sidelobes are achievable after phase error compensation.

Fig. 9 shows the ideal pattern and the measurement patterns before and after correction. Due to the phase errors, there are high levels of sidelobes in the radiation pattern before correction. It is obvious that by applying the corrected phase to the array, the radiation pattern is recovered close to the ideal one. This phase compensation method is proven to be accurate and effective.

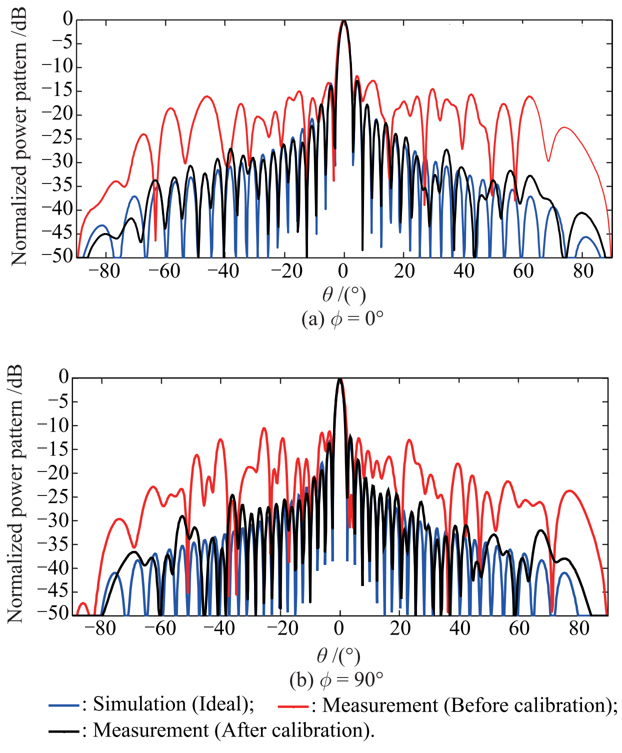

Fig. 9 Measurement results of the radiation pattern before and after correction

Table 4 demonstrates the antenna measured radiation performances before and after correction.

Table 4 Antenna performances before and after phase error correction

Operation	Side-lobe level after correction/dB	First side-lobe before correction/dB	HPBW after correction/(°)
$\phi = 0°$	−12.78/−13.68	−11.78	2.74
$\phi = 90°$	−13.7/−12.3	−11.18	2

6. Conclusions

The phase error correction of a large PAA has been discussed in this paper. At first the analysis of the effect of electrical and mechanical errors on the performance of a PAA has been studied. Then, in order to recover the performance of the PAA in the presence of errors, a phase error correction method using GA has been presented. By using the phase compensation method, the antenna overall radiation pattern has been improved. By applying the simulation data to a 32×40 array of elements with a square grid at the frequency of S-band and the measurement of the radiation pattern, the usefulness of the proposed method has been proved. This approach can be useful for phase error compensation of large phased arrays even with thousands of radiating elements.

References

[1] WANG H S C. Performance of phased-array antennas with mechanical errors. IEEE Trans. on Aerospace and Electronic Systems, 1992, 28(2): 535–545.

[2] WANG C S, KANG M K, WANG W, et al. On the performance of array antennas with mechanical distortion errors considering element numbers. International Journal of Electronics, 2017, 104(3): 462–484.

[3] LIGHTSTONE L. Antenna distortions in multiple phase centre interferometric systems. Proc. of the Geoscience and Remote Sensing Symposium, 1994, 4: 1980–1982.

[4] MAILLOUX R J. Phased array antenna handbook. Boston: Artech House, 2005.

[5] CONGSI W, HONG B, FUSHUN Z, et al. Analysis of electrical performances of planar active phased array antennas with distorted array plane. Journal of Systems Engineering and Electronics, 2009, 20(4): 726–731.

[6] KANG M K, WANG Y, YIN L, et al. Performance prediction for array antennas with element position error based on coupled structural-electromagnetic model. Proc. of the 5th Asia International Symposium on Mechatronics, 2015, 5: 1–5.

[7] WANG Y, WANG C S, YUAN S, et al. Structural-electromagnetic coupling based least squares compensation method for active phased array antenna. Proc. of the 5th Asia International Symposium on Mechatronics, 2015, 6: 1–6.

[8] KANG M K, WANG C S, DUAN B Y, et al. Analysis of influence of array plane error on performances of hexagonal phased array antennas. Proc. of the 31st URSI General Assembly and Scientific Symposium, 2014: 1–4.

[9] WANG C S, KANG M K, WANG W, et al. On the performance of array antennas with mechanical distortion errors considering element numbers. International Journal of Electronics, 2017, 104(3): 462–484.

[10] SON S H, EOM S Y, JEON S I, et al. Automatic phase correction of phased array antennas by a genetic algorithm. IEEE Trans. on Antennas and Propagation, 2008, 56(8): 2751–2754.

[11] BALANIS C A. Antenna theory analysis and design. New York: Wiley, 1997.

Biographies

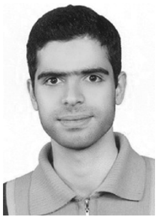

ZAHEDI Amir was born in 1988. He obtained his B.S. degree in electrical engineering from Mehrastan University, Astaneh-ye Ashrafiyeh, Iran and M.S. degree in electrical engineering from Tarbiat Modares University, Tehran, Iran. He has been a member in the Student Activities Committee of the IEEE Iran Section since 2014. His current research interests include antenna and propagation, microwave circuits and optimization methods applied to electromagnetic problems.
E-mail: amir.zahedy@modares.ac.ir

ABBASI ARAND Bijan received his B.S. degree from Shiraz University, Shiraz, Iran in 1995 and M.S. and Ph.D. degrees in telecommunication engineering from Tarbiat Modares University, Tehran, Iran in 1997 and 2003, respectively. From 2003 to 2005, he was a researcher of the Electromagnetic Propagation Department at Iran Telecommunication Research Center (ITRC). In 2005, he joined the Satellite Communication Laboratory of Tarbiat Modares University as a Postdoctoral Researcher. Since 2010, he has been an assistant professor at the Faculty of Electrical and Computer Engineering of Tarbiat Modares University.
E-mail: abbasi@modares.ac.ir